The limiting angles studied in the tests, $\beta = 45, 135°$, are characterized by a sharp fall in heat-transfer intensity. This is due to the fact that as a result of the strong deviation and attenuation of the jet by the induced flow, the jet blowing practically reduces to ventilation of the end gap by air jets.

With increase of Pe (of coolant flow rate) the maximum of heat transfer moves into the zone $\beta < 90°$ (see Fig. 1). This occurs because of an increase of the relative influence of the kinetic energy level of the air jets at the disk surface in the transition from $\beta > 90°$ to $\beta < 90°$ and the increase of the positive radial pressure gradient in the end gap. Tests have shown that with increase of Pe there is an increase of the radial pressure gradient for $\beta < 90°$. The opposite dependence is observed for $\beta > 90°$.

An increase of the positive radial pressure gradient in the flow going out to the disk perimeter promotes turbulence formation in the boundary layer and increased heat transfer.

NOTATION

d, nozzle diameter; R, R_0, ambient radius at the end surface of the disk, and jet inflow radius; z, number of nozzles; U, circumferential velocity at radius R_0; C, velocity of discharge of air from the nozzles; β, angle of the nozzles, formed by the velocity vectors C and U (β = 0 when the directions of the vectors coincide, and β = 180° when the vectors are oppositely directed). Relative quantities are: $X = U/C$; $\bar{d} = d/R_0$; $\bar{R} = R/R_0$. Coefficients are: $\bar{\alpha}$, heat transfer averaged in the jet blowing zone; a, thermal diffusivity; λ, thermal conductivity. Similarity numbers: $Pe = Cd/a$; $\overline{Nu} = \bar{\alpha}d/\lambda$.

LITERATURE CITED

1. Yu. I. Yunkerov, "Results of an investigation of heat transfer on a disk rotating in a housing, with blowing by air jets directed at an arbitrary angle," in: High-Temperature Cooled Aircraft Turbine Engines [in Russian], Kazan Aviation Inst. (1980).
2. B. N. Yudaev, M. S. Mikhailov, and V. K. Savin, Heat Transfer with Interaction of Jets with Obstacles [in Russian], Mashinostroenie, Moscow (1977).
3. B. N. Yudaev, V. N. Dakhno, A. A. Andreev, et al., "An experimental investigation of heat transfer with flow of turbulent jets on to an obstacle," Izv. Vyssh. Uchebn. Zaved., Mashinostr., No. 11, 81 (1971).
4. Yu. V. Ivanov, "Some of the laws for a free circular jet generated in an external transverse flow," Izv. Akad. Nauk SSSR, Otd. Tekh. Nauk, No. 8, 37 (1954).

TURBULENT TWO-PHASE JET AND ITS NUMERICAL INVESTIGATION

L. B. Gavin and V. A. Naumov

UDC 532.529

Using a single-parameter model as a basis, investigators conducted a numerical study of a jet with heavy particles and compared the results with experimental data.

Turbulent jets with heavy particles, characterized by significant nonequilibrium of the flow, have recently become the subject of numerous theoretical [1-5] and experimental [6, 7] studies.

The initial system of equations describing such jet flow can be obtained within the framework of a model of interpenetrating and interacting continua [8] and should be closed with allowance for the effect of the particles on the turbulent structure of the jet. In [1, 4] this closure was effected within the framework of "mixing length" theory in accordance with the recommendations in [2]. Here, in [2, 4], an integral method was used to calculate the two-phase jet. In [1, 5] the finite difference method was used. It should be noted that the Prandtl formulas were replaced in [5] by the eddy viscosity transfer equation of a "pure" gas.

Kalingrad Technical Institute of the Fishing Industry. Translated from Inzhenerno-Fizicheskii Zhurnal, Vol. 44, No. 6, pp. 927–932, June, 1983, Original article submitted January 11, 1982.

0022-0841/83/4406-0623$07.50

To study tubulent jets now, wide use is being made of a method connected with the joint use of the Reynolds equations and equations describing the transfer of the kinetic energy of turbulent pulsations [9]. Among the features of this approach which distinguish it from "mixing length" theory is the possibility of calculating mean parameters and characteristics of turbulence in complicated dissimilar flows with allowance for the flow history and fuller accounting of the external factors. The authors work [3] calculated a two-phase jet using turbulence energy transport equations for a low concentration of drops on the assumption of the absence of mean slip. Here the effect of the drops on the turbulence energy was accounted for approximately by the introduction of empirical corrections to the traditional terms describing turbulence energy generation and dissipation.

The system of equations of an axisymmetric two-phase turbulent jet for mean values has the form

$$\frac{\partial u_g}{\partial x}+\frac{1}{y}\frac{\partial}{\partial y}(yv_g)=0, \tag{1}$$

$$\frac{\partial}{\partial x}(\rho_p u_p)+\frac{1}{y}\frac{\partial}{\partial y}(y(\rho_p v_p+\langle \rho_p' v_p' \rangle))=0, \tag{2}$$

$$\rho_g\left(u_g\frac{\partial u_g}{\partial x}+v_g\frac{\partial u_g}{\partial y}\right)+\frac{1}{y}\frac{\partial}{\partial y}(\rho_g\langle u_g' v_g' \rangle)=-F_x, \tag{3}$$

$$\rho_p u_p\frac{\partial u_p}{\partial x}+(\rho_p v_p+\langle \rho_p' v_p' \rangle)\frac{\partial u_p}{\partial y}+\frac{1}{y}\frac{\partial}{\partial y}(y\rho_p\langle u_p' v_p' \rangle)=F_x, \tag{4}$$

$$u_g\frac{\partial e}{\partial x}+v_g\frac{\partial e}{\partial y}=\frac{1}{y}\frac{\partial}{\partial y}\left(y\frac{\nu_T}{c_q}\frac{\partial e}{\partial y}\right)+\nu_T\left(\frac{\partial u_g}{\partial y}\right)^2-c_D\frac{e^{3/2}}{L}-\varepsilon_p. \tag{5}$$

As in [1, 5], we ignore mean slip in the transverse direction $v_p = v_g = v$. The boundary conditions are:

$$\text{at}\quad y=0\quad \frac{\partial u_g}{\partial y}=\frac{\partial u_p}{\partial y}=\frac{\partial \rho_p}{\partial y}=\frac{\partial e}{\partial y}=v=0, \tag{6}$$

$$\text{at}\quad y=\infty\quad u_g=u_p=u_s,\ \rho_p=\rho_{ps},\ e=e_s. \tag{7}$$

The actual value of the force of phase interaction for spherical particles is

$$\mathbf{F}^*=0.75c_f(\mathbf{V}_g^*-\mathbf{V}_p^*)|\mathbf{V}_g^*-\mathbf{V}_p^*|\rho_g^0\rho_p^*/(\rho_p^0\delta). \tag{8}$$

The drag coefficient, as in [5], is determined from the standard curve of the relation

$$c_f=24(1+0.179\sqrt{\mathrm{Re}^*}+0.013\,\mathrm{Re}^*)/\mathrm{Re}^*. \tag{9}$$

We replace the actual values of the velocities and distributed density by the sum of the mean and pulsative components $\mathbf{V}^* = \mathbf{V} + \mathbf{V}'$, $\rho_p^* = \rho_p + \rho_p'$. Averaging gives us expressions for projections of the mean and pulsative components of the interphase force:

$$F_i=\gamma_y(u_{gi}-u_{pi})\rho_p+\gamma_i\langle(u_{gi}'-u_{pi}')\rho_p'\rangle, \tag{10}$$

$$F_i'=\gamma_i\left((u_{gi}'-u_{pi}')\rho_p+\frac{\gamma_y}{\gamma_i}(u_{gi}-u_{pi})\rho_p'+(u_{gi}'-u_{pi}')\rho_p'-\langle(u_{gi}'-u_{pi}')\rho_p'\rangle\right), \tag{11}$$

$$\gamma_1=\beta(1+0.269\sqrt{\mathrm{Re}}+0.026\,\mathrm{Re}),\ \beta=18\rho_g^0\nu/(\rho_p^0\delta^2), \tag{12}$$

$$\gamma_2=\gamma_3=\beta(1+0.179\sqrt{\mathrm{Re}}+0.013\,\mathrm{Re}). \tag{13}$$

It should be noted that the projections of the mean force on the x axis were introduced into Eqs. (3), (4). Here the second term in Eq. (10) can be ignored compared to the first for flows with a significant mean phase slip.

The last term in (5), present when this equation is derived with allowance for the presence of the phase interaction force in (3), represents the additional dissipation of turbulence energy on the particles and has the form

$$\varepsilon_p \equiv \frac{1}{\rho_g}\sum_i \langle F'_i u'_{gi} \rangle = \frac{1}{\rho_g}\sum_i \gamma_i \left(\langle (u'_{gi} - u'_{pi}) u'_{gi} \rangle \rho_p + \frac{\gamma_y}{\gamma_i}(u_{gi} - u_{pi}) \langle u'_{gi}\rho'_p \rangle + \langle (u'_{gi} - u'_{pi}) u'_{gi}\rho'_p \rangle \right) \quad (14)$$

As the first step in determining ε_p, we omit the triple correlation in (14). The second term can also be omitted, since $u_{gi} = u_{pi}$ when i = 2, 3 and, when i = 1, the correlation moment $\langle u'_{gi}\rho'_p \rangle$, characterizing longitudinal turbulent transport of the mass of the dispersed phase, is small. As a result, we obtain

$$\varepsilon_p = \sum_i \gamma_i (\langle u'^2_{gi} \rangle - \langle u'_{pi} u'_{gi} \rangle) \rho_p/\rho_g. \quad (15)$$

We will write the equation of motion of a single particle [10] in integral form

$$u'_{pi}(t) = u'_{pi}(0)\exp(-\gamma_i t) + \gamma_i \int_0^t \exp(-\gamma_i (t - \tau)) u'_{gi}(\tau)\, d\tau. \quad (16)$$

We multiply both sides of (16) by $u'_{gi}(t)$ and, averaging over the aggregate of particles and time, we obtain

$$\langle u'_{pi}(t) u'_{gi}(t) \rangle = \langle u'_{pi}(0) u'_{gi}(t) \rangle \exp(-\gamma_i t) + \gamma_i \int_0^t \exp(-\gamma_i s) \langle u'_{gi}(\tau) u'_{gi}(\tau + s) \rangle\, ds. \quad (17)$$

The space–time correlation coefficient of the medium along the particle path will be approximated by an exponential relation

$$R_{ij}(s) \equiv \langle u'_{gi}(t) u'_{gj}(t+s) \rangle / \langle u'_{gi}(t) u'_{gj}(t) \rangle = \exp(-\varphi_{ij}|s|). \quad (18)$$

In [10], for the longitudinal and transverse correlations we have

$$\varphi_{11} = (c_\beta \langle u'^2_g \rangle^{1/2} + |u_g - u_p|)/\Lambda_E, \quad \Lambda_E = c_\lambda L, \quad (19)$$

$$\varphi_{22} = \frac{(c_\beta \langle u'^2_g \rangle^{1/2} + |u_g - u_p|)^2}{(c_\beta \langle u'^2_g \rangle^{1/2} + 0.5|u_g - u_p|)\Lambda_E}. \quad (20)$$

Integration of (17) with allowance for (18) gives the following for sufficiently large t:

$$\langle u'_{pi} u'_{gi} \rangle = \langle u'^2_{gi} \rangle \gamma_i/(\gamma_i + \varphi_{ii}). \quad (21)$$

Using the hypothesis of isotropism $\langle u'^2_{gi} \rangle = 2/3$ and inserting (21) into (14), we obtain

$$\varepsilon_p = \frac{2}{3} e \frac{\rho_p}{\rho_g} \sum_i \frac{\gamma_i \varphi_{ii}}{\gamma_i + \varphi_{ii}}. \quad (22)$$

Integrating (16), squaring, and averaging, we write the mean square transverse displacement of the particle [10]

$$\langle r^2_p(t) \rangle = 2 \langle v'^2_g \rangle \left(\frac{t}{\varphi_{22}} - \frac{\gamma_2^2 + \gamma_2\varphi_{22} + \varphi_{22}^2}{\varphi_{22}^2 \gamma_2 (\gamma_2 + \varphi_{22})} - \frac{\varphi_{22}\exp(-\gamma_2 t)}{\gamma_2(\gamma_2^2 - \varphi_{22}^2)} + \frac{\gamma_2^2 \exp(-\varphi_{22} t)}{\varphi_{22}^2(\gamma_2^2 - \varphi_{22}^2)} \right).$$

Since the particle size may be much less than the characteristic hydrodynamic dimension, it can be assumed that the particle moves in a quasiuniform flow. Then the coefficient of transverse diffusion of the particle

$$D_p = 0.5 \lim_{t\to\infty} \frac{d}{dt} \langle r^2_p(t) \rangle. \quad (23)$$

Allowing for (23), we write the expression for the correlation moment, representing the turbulent transport of the mass of the dispersed particles in the transverse direction:

$$\langle \rho'_p v'_p \rangle = -D_p \frac{\partial \rho_p}{\partial y} = -\frac{\langle v'^2_g \rangle}{\varphi_{22}} \frac{\partial \rho_p}{\partial y}. \quad (24)$$

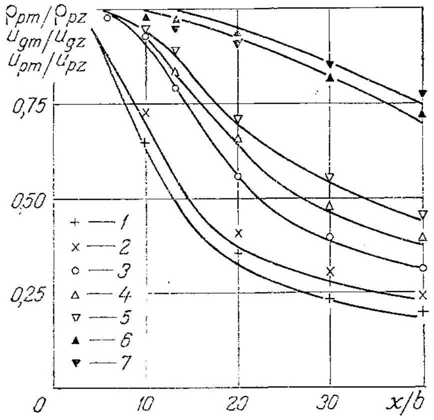

Fig. 1

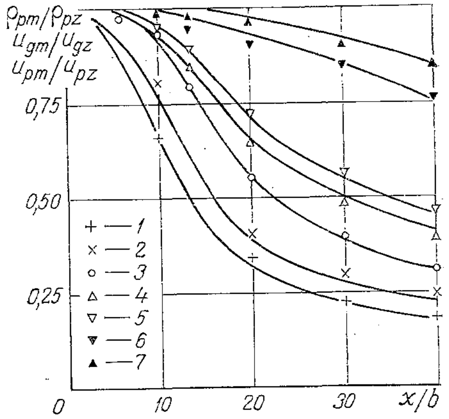

Fig. 2

Fig. 1. Change in the distributed density of the particles and the longitudinal velocities of the gas and particles along the jet axis with $\delta = 45 \cdot 10^{-6}$ m and different initial unit particle flow rates: ρ_{pm}/ρ_{pz} [1) $G_z = 1$; 2) 0.5]; u_{gm}/u_{gz} [3) single-phase jet; 4) $G_z = 0.5$; 5) 1]; and u_{pm}/u_{pz} [6) $G_z = 0.5$; 7) 1].

Fig. 2. Change in the distributed density of the particles and the longitudinal velocities of the gas and particles along the jet axis with $G_z = 1$ and different particle diameters (10^{-6} m): ρ_{pm}/ρ_{pz} [1) $\delta = 45$; 2) 67]; u_{gm}/u_{gz} [3) single-phase jet; 4) $\delta = 67$; 5) 45]; and u_{pm}/u_{pz} [6) $\delta = 45$; 7) 67].

For obtaining the correlation moment $\langle u_p' v_p' \rangle$, we multiply Eq. (13) with i = 1 and j = 2. Then, after averaging, we have the following for sufficiently large t, similar to [11]

$$\langle u_p' v_p' \rangle = \gamma_1 \gamma_2 \int_0^\infty \int_{-\infty}^\infty \exp\left(-(\gamma_1 + \gamma_2) s - \gamma_1 \tau\right) \langle u_g'(t) u_g'(t+s) \rangle \, ds d\tau. \tag{25}$$

Integrating (25) with allowance for (18) gives us

$$\langle u_p' v_p' \rangle = \frac{\gamma_1 \gamma_2}{\gamma_1 + \gamma_2} \left(\frac{1}{\varphi_{12} + \gamma_1} + \frac{1}{\varphi_{12} + \gamma_2} \right) \langle u_g' v_g' \rangle ; \tag{26}$$

we determine $\langle u_g' v_g' \rangle$ from the Kolmogorov hypothesis:

$$\langle u_g' v_g' \rangle = -\nu_t \frac{\partial u_g}{\partial y}, \ \nu_t = c_\nu L \sqrt{e}, \ L = c_L y_u. \tag{27}$$

System of equations (1)-(5), closed with Eqs. (22), (24), (26), (27) and having boundary conditions (6), (7), was solved by the finite difference method using an implicit six-point scheme [12]. The companion flow was assumed to have been equilibrium with respect to velocities. The correspondence for all parameters did not exceed 1%. The accuracy of the calculations was checked by means of integral laws of conservation of excess momentum of a two-phase jet and particle flow rate. As in [7], we took the following for theconditions of discharge and the profiles of u_g, u_p, and ρ_p on the nozzle edge: $u_{gz} = u_{pz} = 35$ m/sec; b = 0.015 m; $\rho_p^\circ = 8500$ kg/m³.

Values of the empirical constants were determined on the basis of the best agreement of the empirical data with different G_z and δ were found to be $c_L = 1.3$; $c_D = 1.0$; $c_q = 0.8$; $c_\nu = 0.08$; $c_\beta = 1.0$; $c_\lambda = 1.0$.

Figures 1-3 compare the results of numerical calculations of the fields of the gas-dynamic parameters of the two-phase jet (curves) with experimental data [7]. Figure 1 shows the distribution the longitudinal velocity of both phases and the distributed density of the dispersed phase on the jet axis for different unit particle flow rates G_z with $\delta = 45 \cdot 10^{-6}$ m.

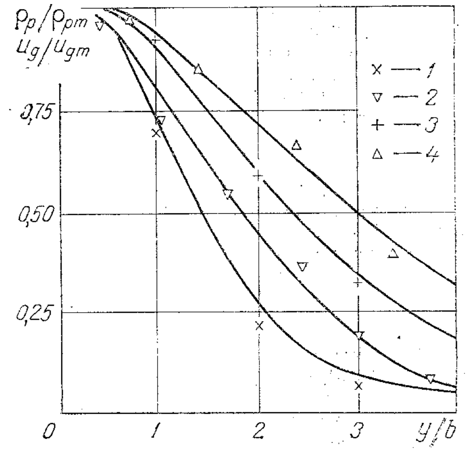

Fig. 3. Profiles of distributed particle density and longitudinal gas velocity in sections: ρ_p/ρ_{pm} [1) x/b = 20; 3) 40]; u_g/u_{gm} [2) x/b = 20; 4) 40]; $\delta = 45 \cdot 10^{-6}$ m, $G_z = 1$.

The numerical studies show that an increase in G_z, as is apparent from (5), results, on the one hand, in a decrease in turbulence energy due to an increase in the additional dissipation in accordance with (22). On the other hand, an increase in G_z increases turbulence energy due to an increase in the production of e, connected with an increase in the transverse velocity gradient of the gas resulting from an increase in the velocity of the carrier phase on the jet axis. It should be noted that turbulence intensity $\sqrt{e}/u_{gm}$ decreases in accordance with the conclusions in [2]. The increase in G_z causes a certain reduction in flow nonuniformity with respect to the velocities of the component phases, as was noted in the experiments in [7]. This leads to an increase in the coefficient of transverse diffusion of the particles in accordance with (20), (24). As a result, ρ_p decreases along the jet axis.

It is apparent that the damping of the axial velocity of the carrier phase depends significantly on the initial particle concentration. With an increase in the latter, there is a decrease in the gas velocity reduction along the jet axis, a result explained not only by an increase in the total surface of the particles and increased phase interaction, but by an increase in additional dissipation of turbulence energy.

Figure 2 shows distributions of u_g, u_p, and ρ_p along the jet axis for different particles sizes with $G_z = 1$. The study results show that an increase in particle size increases flow nonuniformity with respect to velocity, which is explained by a reduction in the interphase surface and, thus, drag. An increase in δ leads to a decrease in u_{gm} and an increase in the gradient $\partial u_g/\partial y$, which in turn causes a reduction in turbulence energy production. Here, in accordance with (22), additional dissipation decreases. As a result, as is evident from (20) and (24), D_p decreases. This leads to a marked increase in the distributed density of the dispersed phase on the jet axis.

Figure 3 shows profiles of the longitudinal velocity of the gas and the distributed density of the dispersed phase across the jet at different stations with $G_z = 1$, $\delta = 45 \cdot 10^{-6}$ m. It is apparent that the fullness of the profiles of u_g is greater than for ρ_p at the respective stations.

The calculated results agree well with the experimental data. Thus, the proposed model can be used in numerical studies of turbulent jets carrying heavy particles.

NOTATION

x, y, coordinates, m; **V**, velocity vector, m/sec; u, v, mean components of velocity along x and y axes, respectively, m/sec; u', v', fluctuation components of velocity, m/sec; δ, particle diameter, m; **F**, force of phase interaction, N; c_f, drag coefficient of particle; Re = $|\mathbf{V}_g - \mathbf{V}_p|\delta/\nu$, Reynolds number; ν, ν_T, kinematic coefficient of molecular and eddy viscosity, m^2/sec; t, τ, s, time, sec; b, nozzle radius, m; ρ°, ρ, true and distributed density, kg/m^3;

e, kinetic energy of turbulent pulsations, m^2/sec^2; ε_p, additional dissipation of turbulence energy, m^2/sec^3; $< r_p^2 >$, mean-square displacement of particle, m^2; L, spatial macroscale, m; Λ_E, Eulerian spatial integral scale, m; $G = \rho_p u_p / \rho_g u_g$, unit particle flow rate; R_{ij}, correlation coefficient; φ_{ij}, exponent; D_p, coefficient of transverse diffusion of particles, m^2/sec; γ_i, β, coefficients, sec^{-1}; y_u, transverse coordinate corresponding to attainment of half the longitudinal velocity of the gas on the jet axis, m; c_L, c_D, c_q, c_ν, c_β, c_λ, empirical constants. Indices: g, p, parameters of the gas and solid phase; z, m, s, parameters of the flow at x = 0, y = 0; y = ∞, respectively; i, j, parameters of the flow pertaining to the i-th and j-th axes; *, actual values of the parameters.

LITERATURE CITED

1. A. P. Vasil'kov, "Calculation of a turbulent two-phase isobaric jet," Izv. Akad. Nauk SSSR Mekh. Zhidk. Gaza, No. 5, 57-63 (1976).
2. G. N. Abramovich and T. A. Girshovich, "Turbulent jets carrying solid or liquid-droplet impurities," in: Vapor–Liquid Flows [in Russian], Nauka i Tekhnika, Minsk (1977), pp. 155-175.
3. H. Danon, M. Wolfshtein, and G. Hetsroni, "Numerical calculation of two-phase turbulent round jet," Int. J. Multiphase Flow, 3, No. 3, 223-234 (1977).
4. A. I. Kartushinskii and F. A. Frishman, "Calculation of the main section of a turbulent two-phase jet," in: Turbulent Two-Phase Flows [in Russian], Izd. Akad. Nauk Estonian SSR, Tallin (1979), pp. 137-141.
5. A. I. Kartushinskii and F. A. Frishman, "Numerical calculation of a turbulent submerged jet," Izv. Akad. Nauk Est. SSR, Fiz. Mat., 29, No. 4, 423-425 (1980).
6. T. A. Girshovich, A. I. Kartushinskii, M. K. Laats, et al., "Study of the effect of impurity concentration and coarseness on the characteristics of a turbulent gas jet with solid particles," in: Investigation of the Working Process in Elements of Motors and Power Plants with a Two-Phase Working Substance [in Russian], Moscow Aviation Inst. (1980), pp. 3-8.
7. T. A. Girshovich, A. I. Kartushinskii, M. K. Laats, et al., "Experimental study of a turbulent jet carrying heavy impurities," Izv. Akad. Nauk SSSR, Mekh. Zhidk. Gaza, No. 5, 26-31 (1981).
8. R. I. Nigmatulin, Principles of the Mechanics of Heterogeneous Media [in Russian], Nauka, Moscow (1978).
9. W. Frost and T. Mauldin (eds.), Turbulence. Principles and Applications [Russian translation], Mir, Moscow (1980).
10. A. A. Shraiber, V. N. Milyutin, and V. P. Yatsenko, Hydromechanics of Two-Component Flows with a Solid Polydisperse Material [in Russian], Naukova Dumka, Kiev (1980).
11. L. M. Pismen and A. Nir, "On the motion of suspended particles in stationary homogeneous turbulence," J. Fluid Mech., 84, No. 1, 193-206 (1978).
12. A. Yu. Brailovskaya and L. A. Chudov, "Solution of boundary-layer equations by a difference method," in: Computing Methods and Programming [in Russian], Moscow State University (1962), pp. 167-182.